Cellular and Molecular Neurobiology
https://doi.org/10.1007/s10571-020-00867-6

ORIGINAL RESEARCH

Synthesis and Characterization of Azido Aryl Analogs of IBNtxA for Radio-Photoaffinity Labeling Opioid Receptors in Cell Lines and in Mouse Brain

Steven G. Grinnell[2,3] · Rajendra Uprety[2] · Andras Varadi[2,3] · Joan Subrath[2] · Amanda Hunkele[2] · Ying Xian Pan[1,2] · Gavril W. Pasternak[1,2,3,4] · Susruta Majumdar[5]

Received: 20 February 2020 / Accepted: 5 May 2020

Abstract

Mu opioid receptors (MOR-1) mediate the biological actions of clinically used opioids such as morphine, oxycodone, and fentanyl. The mu opioid receptor gene, OPRM1, undergoes extensive alternative splicing, generating multiple splice variants. One type of splice variants are truncated variants containing only six transmembrane domains (6TM) that mediate the analgesic action of novel opioid drugs such as 3′-iodobenzoylnaltrexamide (IBNtxA). Previously, we have shown that IBNtxA is a potent analgesic effective in a spectrum of pain models but lacks many side-effects associated with traditional opiates. In order to investigate the targets labeled by IBNtxA, we synthesized two arylazido analogs of IBNtxA that allow photolabeling of mouse mu opioid receptors (mMOR-1) in transfected cell lines and mMOR-1 protein complexes that may comprise the 6TM sites in mouse brain. We demonstrate that both allyl and alkyne arylazido derivatives of IBNtxA efficiently radio-photolabeled mMOR-1 in cell lines and MOR-1 protein complexes expressed either exogenously or endogenously, as well as found in mouse brain. In future, design and application of such radio-photolabeling ligands with a conjugated handle will provide useful tools for further isolating or purifying MOR-1 to investigate site specific ligand–protein contacts and its signaling complexes.

Keywords Photoaffinity labeling · Mu opioid receptor complex · Opioid · IBNtxA · Click · Radioligand binding

Steven G. Grinnell and Rajendra Uprety have contributed equally to this work.

Electronic supplementary material The online version of this article (https://doi.org/10.1007/s10571-020-00867-6) contains supplementary material, which is available to authorized users.

✉ Steven G. Grinnell
Steven.vasquez.grinnell@gmail.com

✉ Susruta Majumdar
susrutam@email.wustl.edu

1 Department of Neurology, Memorial Sloan-Kettering Cancer Center, New York, NY, USA

2 Molecular Pharmacology and Chemistry Program, Memorial Sloan-Kettering Cancer Center, New York, NY, USA

3 Neuroscience Graduate Program, Weill Cornell Graduate School of Medical Sciences, New York, NY, USA

4 Pharmacology Graduate Program, Weill Cornell Graduate School of Medical Sciences, New York, NY, USA

5 Center for Clinical Pharmacology, St Louis College of Pharmacy and Washington University School of Medicine, St Louis, MO, USA

Introduction

Mu opioid receptors (MOR-1) are members of the G-protein coupled receptors (GPCR) family. The gene encoding them, *Oprm1*, generates a range of receptors due to alternative splicing (Pasternak and Pan 2013). As the repertoire of opioid targets has expanded, questions have arisen regarding their detail structure and nature of specific protein–protein interactions responsible for their biological action. A major focus in many of these studies has been the identification and isolation of these targets. One of the robust approaches is to use affinity labeling tools (Bochet et al. 1988; Takayanagi et al. 1982). Affinity labeling is a classical biochemical technique in which a high affinity ligand bearing a reactive group is covalently coupled within its binding pocket (Sumranjit and Chung 2013; Wofsy et al. 1962). Photoaffinity labeling enables a formation of covalent cross-link between the target and the ligand upon brief exposure to ultraviolet (UV) light and the technique can be used to map the binding pocket of the ligand. Rationally designed opioid photoaffinity probes

Published online: 18 May 2020

with a bio-conjugation handle such as alkyne can be radiolabeled that provides a way to follow the target during purification. Next, the alkyne handle can be used to conjugate, through CLICK chemistry, with biotin or peptide epitopes to facilitate the purification of the target protein (Best 2009; Thirumurugan et al. 2013). CLICK chemistry utilizes the highly selective coupling of allylazides with alkynes at room temperature under biologically acceptable conditions. Using CLICK methodology after covalent coupling of an affinity label to its target permits the attachment of a variety of structures that might have interfered with the ability of the affinity probe to label its target. Here, we describe synthesis and in vitro characterization of two new high affinity, high-specific activity, photoactivatable aryl azidoaryl opioid derivatives, closely related analogs of IBNtxA (Grinnell et al. 2014; Majumdar et al. 2011a, b); one of which has an alkyne moiety suitable to CLICK chemistry for photoaffinity probes. Both probes **10** and **17** have high affinity and specificity at opioid receptors and efficiently radio-photolabeled mMOR-1 as well as mouse brain.

Methods

Chemicals

Drugs were obtained from the Research Technology branch of the National Institute on Drug Abuse (Rockville, MD), Tocris Bioscience (Bristol UK), or Cayman Chemical (Ann Arbor, MI).[^{35}S]-GTPγS and Na^{125}I were purchased from Perkin Elmer (Waltham, MA). Miscellaneous chemicals and buffers were obtained from Sigma Aldrich (St. Louis, MO). IBNtxA, IBNalA and ^{125}I-BNtxA were synthesized and structures were confirmed as previously described (Majumdar et al. 2011a, 2012). All non radioactive compounds were dissolved in DMSO and diluted with water for conducting assays. The final concentration of DMSO while conducting the assay was < 1%.

Cell Lines

Chinese hamster ovary (CHO-K1, ATCC® CCL-61™) cells were bought from ATCC. SK-N Be(2)C cells (CCL-2268) obtained from ATCC and CHO-K1 cells were maintained in F12 medium supplemented with 10% fetal bovine serum and minimum Eagle's medium supplemented with 10% fetal bovine serum and F12:nonessential amino acids, respectively, in an atmosphere of 5% CO_2 at 37 °C. The mMOR-1 and mKOR-1 stable line generation used protocols as described previously (Pan 2003). The cDNA fragment containing the full-length mDOR-1 generated by PCR using a mDOR-1/SKII plasmid as the template was subcloned into pcDNA3.1-Hygro vector (Invitrogen), a mammalian expression vector. The resulting plasmid, mDOR-1/pcDNA3.1-Hygro was used to transfect Chinese hamster ovary (CHO-K1, CCL-61, ATCC) cells by LipofectAMINE reagent (Invitrogen). Stable transformants were obtained 2 weeks after selection with hygromycin and screened with [^{3}H]DPDPE binding assay. These cell lines have been previously used in our previous publications (Majumdar et al. 2011a, 2012; Varadi et al. 2016).

Animals

Adult male CD-1 and C57Bl/6 (6–8 weeks old) mice were purchased from Charles River Laboratories. MOR Exon 11 knockout animals were derived as previously described (Pan et al. 2003) and backcrossed at least 10 generations on a C57Bl6/J background. Opioid receptor triple knockout (TKO) animals used were generated in the laboratory of John Pintar (Clarke et al. 2001; Schuller et al. 1999; Zhu et al. 1999) and maintained on an inbred 129S6 background.

All mice were maintained on a 12-h light/dark cycle with Purina rodent chow and water available ad libitum. Mice were housed in groups of five until sacrifice by cervical dislocation. All animal studies were approved by the Institutional Animal Care and Use Committee of Memorial Sloan-Kettering Cancer Center and performed in accordance with the National Institutes of Health Guide for the Care and Use of Laboratory Animals in an Association for Assessment and Accreditation of Laboratory Animal Care accredited facility.

Receptor Binding Studies

^{125}I-IBNtxA and ^{125}I-labeled photoaffinity ligand binding assays were carried out in the homogenate of CHO cells stably expressing mMOR-1, mDOR-1, or mKOR-1 receptors, prepared as described previously (Majumdar et al. 2011a), with 3–10 µg protein in a volume of 1 mL of 50 mM KPO_4 buffer, pH 7.4. Triple knockout mouse brain membrane homogenates were prepared and binding carried out as previously described (Majumdar et al. 2011b) with 200 µg protein in 1 mL of 50 mM KPO_4 with 5 mM $MgSO_4$ buffer. 6TM/E11 competition binding assays using ^{125}I-BNtxA (0.15 nM) were carried out in whole brain membrane homogenates (0.5 ml; 0.5 mg protein) at 25 °C in potassium phosphate buffer (50 mM; pH 7.4) with magnesium sulfate (5 mM) for 90 min in the presence of CTAP, U50488H and DPDPE, all at 200 nM, to block traditional opioid binding sites. Specific binding was defined as the difference between total binding and nonspecific binding, determined in the presence of levallorphan (8 µM) (). K_i values were determined by the following the equation: $K_i = (IC_{50})/(1 + S)$ where S = (concentration of radioligand)/(K, of radioligand) according to the previous report (Cheng and Prusoff 1973; Chou 1974).

Nonspecific binding was determined in the presence of levallorphan (1 μM) and specific binding is reported. For competition and saturation assays, binding was carried out for 90 min at 25 °C to reach equilibrium, then terminated by filtration through Whatman GF/C Glass fiber filters soaked in 0.5% polyethyleneimine for at least 15 min prior to filtration to minimize nonspecific binding to the filters. Filters were then washed with 3 × 2 mL cold buffer (50 mM Tris–HCl, pH 7.4), cut out, and counted on a Perkin Elmer Wizard 1470 gamma counter.

Specific Binding of IBzA

At mMOR-1, 7.5 μg total protein per tube, a maximum of 86.4% of total binding was specific, decreasing to 73.6% at the highest concentration shown as specific binding approached saturation. At mKOR-1, 10 μg total protein per tube, a maximum of 82.6% of total binding was specific, decreasing to 59.2% at the highest concentration shown as specific binding approached saturation.

Specific Binding of Alkynyl-IBzA.

At mMOR-1, 2.5 μg total protein per tube, a maximum of 62.1% of total binding was specific, decreasing to 32.4% at the highest concentration shown as specific binding approached saturation. At mKOR-1, 7.5 μg total protein per tube, a maximum of 62.4% of total binding decreasing to 39.8% at the highest concentration shown as specific binding approached saturation.

Dissociation assays were performed as above except that after 90 min of binding to reach equilibrium, 10 μM levallorphan was added at various time points up to 4 h later to compete radioligand binding and all tubes filtered at the same time. 10 μM levallorphan was used to define nonspecific binding and specific binding is reported.

[^{35}S]GTPγS Functional Assay

[^{35}S]GTPγS binding was performed on membranes prepared from stably opioid receptor transfected cells in the presence and absence of the indicated compound for 60 min at 30 °C in the assay buffer (50 mM Tris–HCl, pH 7.4, 3 mM $MgCl_2$, 0.2 mM EGTA, and 10 mM NaCl) containing 0.05 nM [^{35}S] GTPγS; 2 μg/ml each leupeptin, pepstatin, aprotinin, and bestatin; and 30 μM guanosine diphosphate (GDP), as previously described (Bolan et al. 2004). After the incubation, the reaction was filtered through glass-fiber filters (Whatman Schleicher & Schuell, Keene, NH) and washed three times with 3 mL of ice-cold buffer (50 mM Tris–HCl, pH 7.4) on a semiautomatic cell harvester. Filters were transferred into vials with 3 mL of Liquiscint (National Diagnostics, Atlanta, GA), and the radioactivity in vials was determined by scintillation spectroscopy in a Tri-Carb 2900TR counter (Perkin Elmer Life and Analytical Sciences). Basal binding was determined in the presence of GDP and the absence of drug. Data were normalized to 100 nM DAMGO for mMOR-1. EC_{50} and $\%E_{max}$ values were calculated by nonlinear regression analysis (GraphPad Prism, San Diego, CA).

Photoaffinity Labeling

The indicated ^{125}I-labeled photoaffinity ligand was incubated with 0.5 mg-2 mg protein (mMOR-1) at a final concentration of 0.3–0.5 nM in a volume of 2 mL 50 mM KPO_4 or 50 mM KPO_4/5 mM $MgSO_4$ buffer, pH 7.4, in microcentrifuge tubes for 90 min at 25 °C to reach equilibrium. Tubes were then centrifuged for 10 min at room temperature at 20,000×*g* to separate free ligand and rapidly resuspended in 2 mL ice-cold KPO_4 buffer and transferred to an acrylic cuvette (Nümbrecht, Germany). Photolysis was initiated in a Rayonet photoreactor (RPR-200, Southern New England Ultraviolet Company, Branford CT) equipped with 13 RPR-3500 bulbs for irradiation at 350 nm for 5 min. The photolysate was then transferred back to a microcentrifuge tube, centrifuged at 4 °C for 10 min, and the supernatant discarded. The pellet was then solubilized at 4 °C with either denaturing (radioimmuno precipitation assay buffer, (RIPA)) or nondenaturing (0.2–0.25wt% MNG-3 in 1 × Tris buffered saline; Chae et al. 2010) buffer with EDTA-free HALT protease inhibitor cocktail (containing AEBSF HCl, Aprotinin, Bestatin, E-64, Leupeptin, Pepstatin A; ThermoFisher Scientific, Waltham, MA). The solubilizate was then clarified by centrifugation for 10 min at 4 °C at 20,000×*g*.

The clarified solubilizate was either directly run on a 10% SDS-PAGE gel (BioRad, Berkeley, CA) at 300 V for 19 min following incubation at room temperature for 30 min with Laemmli sample buffer and 5% β-mercaptoethanol or subjected to further purification. BioRad Precision Plus molecular weight markers were used, with MagicMark XP western blot molecular weight markers. Gels were transferred to PVDF in a BioRad Transblot semi-dry transfer device for 7 min at 2.5A and apposed to Koday Biomax MR film with a Kodak Biomax Intensifying Screen at − 80 °C for exposure from 3 h to 8 days.

Wheat germ agglutinin (WGA) affinity purification was performed according to the manufacturer's protocol (Vector Labs, Burlingame, CA). Briefly, 25 μL of a slurry of WGA-agarose beads was transferred to a microcentrifuge tube containing 20 volumes of nondenaturing MNG-3 (maltose lauryl neopentyl glycol, Affymetrix, Santa Clara, CA) buffer and washed 3 times with 20 volumes of fresh non denaturing MNG-3 buffer solution. The clarified solubilizate was added and rotated for 30 min at room temperature before 3 washes with 30 volumes of fresh nondenaturing buffer. The target was then eluted

twice using *N*-acetylglucosamine elution solution (Vector Labs), run through a 7 kDa MWCO Zeba spin desalting column equilibrated with nondenaturing buffer, and concentrated on a 10 kDa NMWL Amicon Ultra 0.5 spin concentrator cartridge to the desired final volume. The final product was incubated at room temperature for 30 min with Laemmli sample buffer and 5% β-mercaptoethanol and separated by SDS-PAGE as above.

Immunoaffinity purification was also performed under both denaturing and nondenaturing conditions, according to manufacturer's protocols. Solubilizate was incubated with rabbit polyclonal antibody directed against the C-terminal tail of the mu opioid receptor (C-20, Santa Cruz Biotechnology, Dallas, TX) according to the manufacturer's suggested dilution relative to the protein added, rotating at 4 °C for 1 h—overnight. Antibody–receptor complexes were then pulled down with Protein A-agarose (EzView Red, Sigma Aldrich) for 1–2 h and equilibrated according to manufacturer's protocols. Beads were washed 2–3 times with 30 volumes buffer until no radioactivity could be detected in the wash with a survey meter. For denaturing conditions, beads were eluted for 30 min with 6.5 M urea, 150 mM DTT, and 1 × Laemmli sample buffer at room temperature and separated by SDS-PAGE as above. For native conditions, beads were eluted 2 times with 100 µg/mL MOR C-20 blocking peptide (Santa Cruz Biotechnology) for 30 min at room temperature. The eluate was then concentrated in a 100 kDa NMWL Millipore Biomax spin concentrator.

Blue Native PAGE

Blue native polyacrylamide gel electrophoresis was performed according to manufacturer's protocols (Life Technologies, Carlsbad, CA), based on the method of Schägger and von Jagow. Briefly, samples were prepared by adding glycerol (10% final concentration) and Coomassie Brilliant Blue G-250 (0.05–0.0625% final concentration). Samples were then loaded onto a 4–16% native gel (Life Technologies) and separated for 105–115 min at 150 V. Gels for imaging were destained in 40% MeOH/10% Acetic Acid solution for 15 min, followed by 8% Acetic acid for 1hour, then imaged on a Chemidoc MP (BioRad). Gels for autoradiography were transferred to PVDF and apposed to film as above.

2D Blue Native/SDS-PAGE was performed by excising a lane from a BN-PAGE gel and incubating at room temperature in 1% SDS/1% β-mercaptoethanol with rocking for 30 min. The highest molecular weight portion of the lane was trimmed to make a 6 cm strip for insertion into a Life Technologies NuPage Novex 12% Bis–Tris gel with a 2D well. Gels were run with MOPS-SDS buffer for 1 h at 200 V per manufacturer's protocol, then transferred to PVDF and apposed to film with an intensifying screen as above.

Synthesis of compounds

All chemicals were purchased from Sigma Aldrich Chemicals and Alfa Aesar, and were used without further purification. Reaction mixtures were purified by Silica Flash chromatography on E. Merck 230–400 mesh silica gel 60 using a Teledyne ISCO CombiFlash R_f instrument with UV detection at 280 nm and 254 nm. RediSep R_f silica gel normal phase columns were used with a gradient of MeOH in DCM or EtOAc in hexanes. The yields reported are isolated yields. IR spectra were recorded on a Bruker Optics Tensor 27 FTIR spectrometer with peaks reported in cm^{-1}. NMR spectra were recorded on Bruker Avance III 500, Avance III 600 with DCH CryoProbe instruments. NMR spectra were processed with MestReNova software (ver. 6.1.1.). Chemical shifts are reported in parts per million (ppm) relative to residual solvent peaks rounded to the nearest 0.01 for proton and 0.1 for carbon ($CDCl_3$ ^1H: 7.26, ^{13}C: 77.1; CD_3OD ^1H: 3.31, ^{13}C: 49.0; DMSO-d_6 ^{13}C: 39.5). Peak multiplicity is reported as follows: s—singlet, d—doublet, t—triplet, q—quartet, m—multiplet. Coupling constants (*J*) are expressed in Hz. Mass spectra were obtained at the MSKCC Analytical Core Facility on a Waters Acuity SQD LC–MS by electrospray (ESI) ionization. High resolution mass spectra were obtained on a Waters Acuity Premiere XE TOF LC–MS by electrospray ionization. Accurate masses are reported for the molecular ion $[M+H]^+$. HPLC: Waters 1525 Binary Pump, Waters 2489 UV/vis Detector, Waters XBridge C18 column (5 µm × 150 × 4.6 mm), mobile phase: solvent A: water with 0.1% TFA; aolvent B: acetonitrile with 0.1% TFA. Gradient: 5–95% acetonitrile/water. Flow rate: 1 ml/min. A reversed-phase HPLC using a Perkin Elmer LC pump series 200 and a 785A UV/vis detector (214 nM) was used. A Varian microsorb MV 100 − 5 reversed-phase column (5 µm × 4.6 mm × 250 mm) with the mobile phases being 0.1% TFA in water and 0.1% TFA in ACN with a gradient elution at a flow rate of 1 mL/min was used.

Ethyl 4-amino-3-iodobenzoate (2)

Concentrated sulfuric acid (a catalytic amount, one drop) was added to a stirred solution of ethyl 4-amino benzoate **1** (1 g, 6.05 mmol) dissolved in acetonitrile (17 mL) at room temperature. *N*-iodosuccinimide (1.5 g 6.66 mmol) was added to the reaction mixture. After stirring for 2 h at rt, the reaction mixture was quenched with phosphate buffer (pH 7.4, 17 mL). Then, the product was extracted in EtOAc (50 mL). The EtOAc layer was dried over anhydrous Na_2SO_4, filtered, concentrated under reduced pressure; and dried under high vacuum to get desired product **2** (1.38 g;

yield 79%). ^{1}H NMR (500 MHz, $CDCl_3$): $\delta = 8.32$ (s, 1H), 7.81 (d, $J = 5.1$ Hz, 1H), 6.69 (d, $J = 4.2$ Hz, 1H), 4.51 (br, 2H), 4.31 (m, 2H), 1.36 (t, $J = 7.1$ Hz, 3H).

Ethyl 4-azido-3-iodobenzoate (3)

Concentrated hydrochloric acid (4 mL, 12 M) was added drop wise to the stirred solution of ethyl amino benzoate **2** (1.1 g, 3.8 mmol) in MeOAc (12 mL) at rt. over a period of 2 min. The reaction mixture was cooled to 4 °C. Aqueous solution (2.5 mL) of $NaNO_2$ (780 mg, 11.3 mmol) was added to the mixture and the reaction continued for 45 min in dark (covered with an aluminum foil) at the temperature. Then, NaN_3 (784 mg, 12.1 mmol) was added to the reaction mixture in portions for period of 15 min. After stirring the reaction mixture for additional 15 min, the reaction mixture was quenched with phosphate buffer (pH 7, 25 mL). Then, the product was extracted in EtOAc (50 mL). The EtOAc layer was dried over anhydrous Na_2SO_4, filtered, concentrated under reduced pressure; and dried under high vacuum to get desired product **3** (1.0 g; yield 83%). ^{1}H NMR (500 MHz, $CDCl_3$): $\delta = 8.45$ (s, 1H), 8.05 (d, $J = 5.1$ Hz, 1H), 7.16 (d, $J = 4.1$ Hz, 1H), 4.36 (m, 2H), 1.39 (t, $J = 7.1$ Hz, 3H).

4-Azido-3-iodobenzoic acid (4)

Aqueous solution (500 µL) of lithium hydroxide (22 mg, 0.94 mmol) was added to the stirred solution of ethyl ester **3** (100 mg, 0.31 mmol) dissolved in MeOH: THF (1:1) mixture (1 mL) at rt. The reaction mixture was continued overnight. TLC indicated the completion of ester hydrolysis. Then, the reaction mixture was concentrated under reduced pressure to remove organic solvents and the remaining content was diluted with water (5 mL). The aqueous layer was acidified (pH 3) with dilute HCl and diluted with brine (10 mL). Then, the product was extracted in DCM (2 × 10 mL), the DCM layer was dried over anhydrous Na_2SO_4, and filtered. The filtrate was concentrated under reduced pressure and dried under high vacuum to get brown solid **4** (89 mg; quantitative yield; used without further purification for the next step). ^{1}H NMR (500 MHz, $CDCl_3$): $\delta = 8.52$ (s, 1H), 8.11 (d, $J = 5.1$ Hz, 1H), 7.20 (d, $J = 4.1$ Hz, 1H).

Ethyl 4-azido-3-(tributylstannyl)benzoate (5)

Bis(tributyltin) (320 µL, 0.63 mmol) was added to the stirred solution of 3-iodo 4-azido ethyl ester **4** (50 mg, 0.15 mmol) dissolved in dry dioxane (2 mL) under argon atmosphere at rt. Pd $(PPh_3)_4$ (18 mg, 0.015 mmol) was added to the mixture at rt; and the reaction mixture was heated to reflux overnight. TLC (using silica plate with developing solvent 1% EtOAc in hexanes) indicated the complete consumption of starting material. Then, the reaction mixture was cooled to rt, diluted with 5%EtOAc in hexanes (15 mL); and the mixture was filtered through celite. The filtrate was concentrated under reduced pressure and the residue was purified by silica column chromatography (ISCO, 4 g) using 0–1% EtOAc in hexanes. The desired product fractions (26–27 tubes) were combined, concentrated under reduced pressure; and dried under high vacuum to get a colorless oil **5** (18 mg; yield 25%). ^{1}H NMR (500 MHz, $CDCl_3$): $\delta = 8.07$ (s, 1H), 8.01 (d, $J = 5.1$ Hz, 1H), 7.16 (d, $J = 4.1$ Hz, 1H), 4.38–4.34 (m, 2H), 1.54–1.40 (m, 6H), 1.39–1.30 (m, 10H), 1.13–1.09 (m, 5H), 0.2–0.87 (m 9H).

4-Azido-3-(tributylstannyl)benzoic Acid (6)

Aqueous potassium hydroxide (0.03 mmol, 200 µL) was added to the stirred solution of tributyl tin azido ethyl ester **5** (10 mg, 0.02 mmol) dissolved in MeOH (1 mL) at rt. The reaction mixture was heated to 60 °C overnight. TLC indicated the completion of ester hydrolysis. Then, the reaction mixture was cooled to rt and concentrated under the reduced pressure. Then, the residue was diluted with DCM (20 mL), and saturated solution of NH_4Cl (10 mL) was added into it. The DCM layer was separated and was washed with brine (10 mL), dried over anhydrous Na_2SO_4; and filtered. The filtrate was concentrated under reduced pressure and dried under high vacuum to get colorless oil **6** (7 mg; yield 77%).^{1}H NMR (500 MHz, $CDCl_3$): $\delta = 8.13$ (s, 1H), 8.08 (d, $J = 4.1$ Hz, 1H), 7.19 (d, $J = 4.1$ Hz, 1H), 1.15–1.34 (m, 5H), 1.32–1.29 (m, 8H), 1.14–1.11 (m, 5H), 0.93–0.87 (m, 9H).

N-((4*R*,4*aS*,7*R*,7*aR*,12*bS*)-3-Allyl-4*a*,9-dihydroxy-2,3,4,4*a*,5,6,7,7a-octahydro-1H-4,12-methanobenzofuro[3,2-e] isoquinolin-7-yl)-4-azido-3-(tributylstannyl)benzamide (9)

DIPEA (27.0 µL, 0.154 mmol) and ally amine **8** (10.0 mg, 0.030 mmol) were added to the stirred solution of azide acid **6** (14.0 mg, 0.030 mmol) dissolved in DMF (700 µL) at rt under Argon atmosphere. The reaction mixture was cooled to 0 °C and HATU (11.7 mg, 0.030 mmol) was added to the reaction mixture. After stirring the reaction mixture for 3 h at 0 °C to rt., the reaction mixture was poured into EtOAc (20 mL) and was washed with brine (7 × 15 mL). The EtOAc layer was dried over Na_2SO_4, filtered; and concentrated under reduced pressure. Then, the residue was redissolved in MeOH (2 mL), and treated with NaOMe in methanol (0.5 M, 150 µL), for one hour at rt. Finally, the reaction mixture was concentrated under reduced pressure, and the residue was purified by silica gel column chromatography (ISCO, 4 g) using 5–10% MeOH in DCM. The desired product fractions were concentrated under reduced pressure and dried under high vacuum to get desired product **9** (10 mg; Yield 45%); ^{1}H NMR (600 MHz, $CDCl_3$) δ 7.97–7.75 (m, 2H), 7.32 (s, 1H), 7.16 (d, $J = 8.1$ Hz, 1H), 6.75 (d,

$J = 8.1$ Hz, 1H), 6.59 (d, $J = 8.1$ Hz, 1H), 5.81 (s, 1H), 5.21 (d, $J = 25.5$ Hz, 2H), 4.52 (s, 1H), 4.29 (s, 1H), 3.21–3.06 (m, 3H), 2.97 (s, 1H), 2.70–2.53 (m, 2H), 2.27–2.21 (m, 2H), 1.66 (d, $J = 33.9$ Hz, 4H), 1.57–1.47 (m, 6H), 1.37–1.27 (m, 6H), 1.16–1.10 (m, 6H), 0.89 (t, $J = 7.4$ Hz, 12H). ^{13}C NMR (151 MHz, $CDCl_3$) δ 149.25, 143.60, 136.34, 135.07, 130.54, 129.10, 119.36, 116.80, 93.14, 70.32, 62.59, 60.57, 57.93, 49.61, 47.20, 38.77, 31.75, 29.17, 27.47, 22.82, 14.29, 13.89, 10.36. HRMS: *m/z* calcd for $C_{38}H_{53}N_5O_4Sn$ $[M+H]^+$: 764.3198; found 764.3212; purity > 95% by HPLC.

***N*-((4*R*,4*aS*,7*R*,7*aR*,12*bS*)-3-Allyl-4*a*,9-dihydroxy-2,3,4,4*a*,5,6,7,7a-octahydro-1H-4,12-methanobenzofuro[3,2-e]isoquinolin-7-yl)-4-azido-3-iodobenzamide (10)**

DIPEA (11.2 µL, 0.064 mmol) and allyl amine **8** (7.0 mg, 0.021 mmol) were added to the stirred solution of azide acid **4** (12.3 mg, 0.042 mmol) dissolved in DMF (700 µL) at rt under an argon atmosphere. The reaction mixture was cooled to 0 °C and HATU (16.3 mg, 0.064 mmol) was added to the reaction mixture. After stirring the reaction mixture for 2 h at 0 °C to rt., the reaction mixture was poured into EtOAc (20 mL) and was washed with brine (7 × 15 mL). The EtOAc layer was dried over Na_2SO_4, filtered; and concentrated under reduced pressure. Then, the residue was redissolved in MeOH (2 mL), and treated with NaOMe in methanol (0.5 M, 150 µL), for one hour at rt. Finally, the reaction mixture was concentrated under reduced pressure, and the residue was purified by silica gel column chromatography (ISCO, 4 g) using 5–10% MeOH in DCM. The desired product fractions were concentrated under reduced pressure and dried under high vacuum to get desired product **10** (8.0 mg; Yield 64%); ^{1}H NMR (600 MHz, $CDCl_3$) $\delta = 7.84$ (dd, $J = 8.3$, 2.0 Hz, 1H), 7.44 (d, $J = 8.9$ Hz, 1H), 7.09 (d, $J = 8.3$ Hz, 1H), 6.61 (dd, $J = 57.6$, 8.1 Hz, 2H), 5.90–5.69 (m, 1H), 5.25–5.11 (m, 2H), 4.64 (d, $J = 5.9$ Hz, 1H), 4.06–4.03 (m, 1H), 3.18–3.07 (m, 3H), 2.97 (q, $J = 8.4$, 7.0 Hz, 1H), 2.67–2.51 (m, 2H), 2.19 (d, $J = 7.4$ Hz, 2H), 1.99–1.89 (m, 1H), 1.69–1.65 (m, 1H), 1.62–1.56 (m, 1H), 1.52–1.41 (m, 2H), 1.29–1.21 (m, 1H). ^{13}C NMR (151 MHz, $CDCl_3$) $\delta = 142.82$, 139.08, 132.29, 130.67, 128.61, 119.50, 117.99, 117.72, 92.68, 87.59, 70.48, 62.53, 57.92, 50.91, 47.39, 43.73, 31.59, 29.35, 23.45, 22.85, 14.35. HRMS: *m/z* calcd for $C_{26}H_{26}N_5O_4I$ $[M+H]^+$: 600.1108; found 600.1084; purity > 97% by HPLC.

(4R,4aS,7aR,12bS)-4a,9-Dihydroxy-2,3,4,4a,5,6-hexahydro-1H-4,12-methanobenzofuro[3,2-e]isoquinolin-7(7aH)-one (11)

Dissolved naloxone (**7**, 15 g, 45.82 mmol) in dry DCM (110 mL), then a solution of N,N-dimethyl barbituric acid (4.29 g, 27.49 mmol, 0.6 eq.) and $Pd(PPh_3)_4$ (2.65 g, 2.29 mmol, 0.05 eq.) in dry DCM (190 mL) was added and 38 °C under Ar for 16 h. The cooling to rt, the mixture was filtered and washed with cold DCM, then water. The solid was dissolved in a mixture of water and conc. aq. HCl (7:1, 480 mL) at 40 °C. The aqueous layer was washed with DCM, then it was basified to pH ~ 9 with ammonia. The resulting solid was filtered and dried under high vacuum to yield 11 as a light orange solid (10.98 g; Yield: 83%). ^{1}H NMR (600 MHz, Methanol-d_4) δ 6.65 (d, $J = 8.1$ Hz, 1H), 6.62 (d, $J = 8.0$ Hz, 1H), 4.69 (s, 1H), 3.13 (d, $J = 6.1$ Hz, 1H), 3.10–2.98 (m, 3H), 2.80 (dd, $J = 13.4$, 4.5 Hz, 1H), 2.57 (td, $J = 13.0$, 3.6 Hz, 1H), 2.50 (td, $J = 12.4$, 4.6 Hz, 1H), 2.26–2.18 (m, 1H), 1.88–1.77 (m, 1H), 1.62 (td, $J = 14.2$, 3.4 Hz, 1H), 1.39 (dd, $J = 12.3$, 3.5 Hz, 1H).

(4*R*,4*aS*,7*aR*,12*bS*)-4*a*,9-Dihydroxy-3-(prop-2-yn-1-yl)-2,3,4,4*a*,5,6-hexahydro-1H-4,12-methanobenzofuro[3,2-e]isoquinolin-7(7*a*H)-one (12)

Sodium carbonate (370.4 mg, 3.49 mmol) and propargyl bromide (389 µL, 3.49 mmol, 80% in toluene) were added to a stirred solution of noroxymorphone **11** (1 g, 3.48 mmol) dissolved in anhydrous DMF (5 mL) at rt. under an argon atmosphere. The reaction mixture was heated to 90 °C overnight. Mass spectrometry of the crude reaction mixture indicated the completion of the reaction. The solvent was removed under reduced pressure and the residue was redissolved in EtOAc (50 mL). The EtOAc layer was washed with brine (5 × 30 mL), dried over anhydrous Na_2SO_4, filtered, and concentrated under reduced pressure. The crude product was purified by silica gel column chromatography (ISCO-combiflash) using 1–5% MeOH in DCM. The desired product fractions were concentrated under reduced pressure and dried under high vacuum to obtain off-white solid **12** (897 mg; yield 78%). ^{1}H NMR (600 MHz, $CDCl_3$ + MeOH) $\delta = 7.92$–7.76 (m, 1H), 7.26 (dd, $J = 8.5$, 4.4 Hz, 1H), 7.15 (t, $J = 7.2$ Hz, 1H), 5.25–5.06 (m, 1H), 3.95 (dd, $J = 8.3$, 4.0 Hz, 2H), 3.80–3.65 (m, 2H), 3.65–3.49 (m, 1H), 3.25–3.10 (m, 2H), 2.99–2.78 (m, 4H), 2.54–2.39 (m, 1H), 2.20–2.12 (m, 2H).

(4*R*,4*aS*,7*S*,7*aR*,12*bS*)-3-(Prop-2-yn-1-yl)-1,2,3,4,5,6,7,7*a*-octahydro-4*a*H-4,12-methanobenzofuro[3,2-e]isoquinoline-4*a*,7,9-triol (13)

K-Selectride (5.2 mL, 5.22 mmol, 1 M in THF) was slowly added to a stirred solution of ketone **12** (850 mg, 2.61 mmol) dissolved in anhydrous THF (20 mL) at 0 °C under an argon atmosphere and the reaction was continued for 30 min at the temperature. Then, the reaction mixture was warmed to rt. and continued overnight. Mass spectrometry of the crude reaction mixture indicated the

completion of the reaction. The reaction mixture was cooled to 0 °C and water (10 mL) was slowly added to quench the reaction. The reaction mixture was stirred for 10 min at rt. Then, the solvent was removed under reduced pressure and the remaining content was diluted with brine (30 mL). The aqueous layer was extracted with DCM (5 × 30 mL). The combined DCM layer was dried over anhydrous Na_2SO_4, filtered, and concentrated under reduced pressure. The crude product was purified by silica gel column chromatography (ISCO-combiflash) using 1–5% MeOH in DCM. The desired product fractions were combined, concentrated under reduced pressure; and dried under high vacuum to obtain white solid **13** (730 mg; yield 85%). ^{1}H NMR (600 MHz, $CDCl_3$) $\delta = 6.71$ (d, $J = 8.1$ Hz, 1H), 6.55 (d, $J = 8.2$ Hz, 1H), 4.67 (d, $J = 4.6$ Hz, 1H), 4.26 (d, $J = 11.2$ Hz, 1H), 3.34 (d, $J = 3.3$ Hz, 2H), 3.22–2.97 (m, 2H), 2.72–2.56 (m, 2H), 2.38 (td, $J = 12.1$, 3.7 Hz, 1H), 2.27 (t, $J = 2.5$ Hz, 1H), 1.79–1.56 (m, 3H), 1.46 (ddd, $J = 14.6$, 8.6, 3.2 Hz, 1H), 1.21–1.03 (m, 1H).

2-((4*R*,4*aS*,7*R*,7*aR*,12*bS*)-4*a*,9-Dihydroxy-3-(prop-2-yn-1-yl)-2,3,4,4*a*,5,6,7,7*a*-octahydro-1H-4,12-methanobenzofuro[3,2-e]isoquinolin-7-yl)isoindoline-1,3-dione (14)

Phthalimide (594.7 mg, 4.04 mmol) and triphenylphosphine (1.06 g, 4.04 mmol) were added to a stirred solution of opiate alcohol **13** (661 mg, 2.02 mmol) dissolved in anhydrous THF (16 mL) at rt. under an argon atmosphere. A solution of diisopropyl azodicarboxylate (795.8 µl, 4.042 mmol) in toluene (1.5 mL) was added drop wise to the reaction mixture and the reaction was continued overnight. Water (3 mL) was added to the reaction mixture and the resulting in mixture was stirred for 10 more minutes. The volatilities were removed under reduced pressure. Aqueous citric acid (2%, 18 mL) and dilute HCl (0.1 M, 6 mL) were added to the crude mixture and the resulting aqueous layer was washed with EtOAc (3 × 20 mL) to remove excess of reagent and the by other products. Then, the aqueous layer was basified (pH 10) with aqueous ammonia (10% NH_4OH), and the mixture was extracted with DCM (3 × 20 mL). The combined DCM layer was dried over anhydrous Na_2SO_4, filtered, and concentrated under reduced pressure. The crude product was purified by silica gel column chromatography (ISCO-combiflash, 220 g) using 20% hexanes in EtOAc (six column volume; to elute impurities) and then with 3–10% MeOH in DCM to elute the desired product. The desired product fractions were combined, concentrated under reduced pressure; and dried under high vacuum to obtain off-white solid **14** (646 mg; yield 70%). ^{1}H NMR (600 MHz, $CDCl_3$) $\delta = 7.85$ (dd, $J = 5.4$, 3.0 Hz, 2H), 7.72 (dd, $J = 5.5$, 3.0 Hz, 2H), 6.77 (d, $J = 8.1$ Hz, 1H), 6.64 (d, $J = 8.0$ Hz, 1H), 5.18 (d, $J = 8.3$ Hz, 1H), 4.70 (s, 2H), 4.06 (ddd, $J = 12.9$, 8.3, 4.4 Hz, 1H), 3.39 (s, 2H) 3.24–3.10 (m, 2H), 2.81 (dd, $J = 13.3$, 2.8 Hz, 1H), 2.74–2.58 (m, 2H), 2.42–2.21 (m, 3H), 1.79–1.68 (m, 1H), 1.54–1.41 (m, 3H).

(4*R*,4*aS*,7*R*,7*aR*,12*bS*)-7-Amino-3-(prop-2-yn-1-yl)-1,2,3,4,5,6,7,7a-octahydro-4*a*H-4,12-methanobenzofuro[3,2-e]isoquinoline-4*a*,9-diol (15)

The *cis*-2-penten-1-ol (2.2 mL, 21.03 mmol) and hydrazine hydrate (819 µl, 13.15 mmol; 50% hydrazine solution) were added to a stirred solution of opiate phthalimides **14** (600 mg, 1.34 mmol) dissolved in MeOH (16 mL) at rt. and the reaction was continued overnight. Mass spectrometry of the crude reaction mixture indicated the completion of the reaction. The volatilities were removed under reduced pressure and the reaction mixture was treated with dilute acetic acid (20 mL, 1.5 M) and filtered. The filtrate was basified (pH 10) with aqueous ammonia (10% NH_4OH), and the mixture was extracted with DCM (3 × 20 mL). The combined DCM layer was dried over anhydrous Na_2SO_4, filtered, and concentrated under reduced pressure. The crude product was purified by silica gel column chromatography (ISCO-combiflash) using 5–15% MeOH in DCM. The desired product fractions were combined, concentrated under reduced pressure; and dried under high vacuum to obtain white solid **15** (353.8 mg; Yield 82%). ^{1}H NMR (600 MHz, $CDCl_3$) $\delta = 6.63$ (d, $J = 8.1$ Hz, 1H), 6.56 (s, 1H), 4.26 (d, $J = 7.0$ Hz, 1H), 3.35 (d, $J = 2.5$ Hz, 2H), 3.16–3.00 (m, 2H), 2.67–2.52 (m, 3H), 2.31–2.09 (m, 3H), 1.79 (tt, $J = 9.7$, 4.6 Hz, 2H), 1.62 (dt, $J = 13.3$, 3.3 Hz, 1H), 1.46–1.34 (m, 2H).

4-Azido-N-((4aS,7R,12bS)-4a,9-dihydroxy-3-(prop-2-yn-1-yl)-2,3,4,4a,5,6,7,7a-octahydro-1H-4,12-methanobenzofuro[3,2-e]isoquinolin-7-yl)-3-(tributylstannyl) benzamide (16)

DIPEA (8.0 µL, 0.046 mmol) and alkyne amine **5** (5.5 mg, 0.017 mmol) were added to the stirred solution of azide acid **6** (7 mg, 0.015 mmol) dissolved in DMF (300 µL) at rt under an argon atmosphere. The reaction mixture was cooled to 0 °C and HATU (6.4 mg, 0.017 mmol) was added to the reaction mixture. After stirring the reaction mixture for 2 h at 0 °C to rt., the reaction mixture was poured into EtOAc (20 mL) and was washed with brine (5 × 15 mL). The EtOAc layer was dried over Na_2SO_4, filtered; and concentrated under reduced pressure. Then, the residue was redissolved in MeOH (2 mL), and treated with NaOMe in methanol (0.5 M, 150 µL), for one hour at rt. Finally, the reaction mixture was concentrated under reduced pressure, and the residue was purified by silica gel column chromatography (ISCO, 4 g) using 0–5% MeOH in DCM. The desired product fractions (21–22 tubes) were concentrated under

reduced pressure and dried under high vacuum to get colorless viscous oil **16** (5.1 mg; Yield 45%); ^{1}H NMR (600 MHz, $CDCl_3$) δ 7.85–7.80 (m, 2H), 7.16 (d, J = 8.2 Hz, 1H), 6.75 (d, J = 8.1 Hz, 1H), 6.59 (d, J = 8.1 Hz, 1H), 5.34 (s, 1H), 5.02 (s, 1H), 4.53 (d, J = 5.0 Hz, 1H), 4.28 (d, J = 4.8 Hz, 1H), 3.42–3.31 (m, 2H), 3.18 (d, J = 18.0 Hz, 2H), 2.74–2.61 (m, 2H), 2.39–2.20 (m, 3H), 1.84 (s, 1H), 1.67 (s, 2H), 1.60–1.49 (m, 7H), 1.33 (dt, J = 14.6, 7.3 Hz, 7H), 1.15–1.08 (m, 6H), 0.89 (t, J = 7.3 Hz, 9H). ^{13}C NMR (151 MHz, $CDCl_3$) δ = 166.62, 149.26, 143.60, 135.10, 130.54, 129.08, 119.40, 117.69, 116.80, 93.12, 70.40, 62.64, 49.65, 47.05, 44.25, 29.24, 27.48, 23.05, 13.90, 10.36. HRMS: *m/z* calcd for $C_{38}H_{51}N_5O_4Sn$ $[M+H]^+$: 762.3041; found 762.3058; purity > 99% by HPLC.

4-Azido-*N*-((4*R*,4a*S*,7*R*,7a*R*,12b*S*)-4a,9-dihydroxy-3-(prop-2-yn-1-yl)-2,3,4,4a,5,6,7,7a-octahydro-1H-4,12-methanobenzofuro[3,2-e]isoquinolin-7-yl)-3-iodobenzamide (17)

DIPEA (11.2 µL, 0.064 mmol) and alkyne amine **15** (7.0 mg, 0.021 mmol) were added to the stirred solution of azide acid **4** (12.3 mg, 0.042 mmol) dissolved in DMF (700 µL) at rt under an argon atmosphere. The reaction mixture was cooled to 0 °C and HATU (16.3 mg, 0.064 mmol) was added to the reaction mixture. After stirring the reaction mixture for 2 h at 0 °C to rt., the reaction mixture was poured into EtOAc (20 mL) and was washed with brine (7 × 15 mL). The EtOAc layer was dried over Na_2SO_4, filtered; and concentrated under reduced pressure. Then, the residue was redissolved in MeOH (2 mL), and treated with NaOMe in methanol (0.5 M, 150 µL), for one hour at rt. Finally, the reaction mixture was concentrated under reduced pressure, and the residue was purified by silica gel column chromatography (ISCO, 4 g) using 4–10% MeOH in DCM. The desired product fractions were concentrated under reduced pressure and dried under high vacuum to get desired product **17** (8.2 mg; yield 66%); ^{1}H NMR (600 MHz, $CDCl_3$) δ = 7.84 (d, J = 8.3, Hz, 1H), 7.38 (d, J = 8.9 Hz, 1H), 7.17–7.03 (m, 1H), 6.67 (d, J = 8.1 Hz, 1H), 6.57 (d, J = 8.2 Hz, 1H), 6.21 (br, 1H), 5.04 (br, 1H), 4.63 (d, J = 5.9 Hz, 1H), 4.06 (dt, J = 9.2, 4.9 Hz, 1H), 3.37 (d, J = 2.4 Hz, 2H), 3.27–3.07 (m, 2H), 2.74–2.56 (m, 2H), 2.40–2.14 (m, 4H), 1.94 (dt, J = 14.2, 4.8 Hz, 1H), 1.71 (dt, J = 13.9, 5.1 Hz, 1H), 1.64–1.57 (m, 1H), 1.57–1.51 (m, 1H), 1.50–1.45 (m, 1H). ^{13}C NMR (151 MHz, $CDCl_3$) δ = 144.79, 142.87, 139.55, 139.07, 132.28, 130.51, 128.59, 119.54, 118.00, 117.79, 92.69, 87.60, 77.37, 73.45, 70.53, 62.58, 50.82, 47.21, 31.40, 29.27, 23.39, 23.16. HRMS: *m/z* calcd for $C_{26}H_{24}N_5O_4I$ $[M+H]^+$: 598.0951; found 598.0937; purity > 95% by HPLC.

Results and Discussion

Chemistry

The design of new radioiodinated photoaffinity labels, **10** and **17** is based on the potent opioid analgesic compounds IBNtxA and its allyl analog IBNalA (Fig. 1) that we had reported before (Majumdar et al. 2012). In case of IBNalA analog, the *N*-cyclopropyl methyl (CPM) group of IBNtxA was swapped with a *N*-allyl group commonly seen in the naloxone scaffold. This small change in structure led to greater selectivity in binding assays for mMOR-1 as well as 6TM/E11 over mDOR-1 when compared to IBNtxA (see Table 1).

We designed our affinity label namely IBzA **10**, incorporating an azido group ortho to the 3′-iodo group of IBNalA and alkynyl-IBzA **17**, where the N-allyl group of **10** is substituted with a N-alkynyl group so that it is available for click chemistry approaches later on for follow up work.

The synthesis of the azido aryl photoaffinity opioid probes, namely IBzA **10**, alkynyl-IBzA **17** and the stannylated precursors to the corresponding radiolabelled ^{125}I compounds **18** and **19** was proceeded with naloxone as a starting material (Scheme 1). 4-Azido-3-iodobenzoic acid (**4**) and 4-azido-3-(tributylstannyl)benzoic acid (**6**) were prepared from ethyl-4-amino benzoate **1**. Iodination of **1** with *N*-iodosuccinimide and subsequent diazotization of the amine **2** in acidic conditions followed by nucleophilic substitution with an azide resulted in ethyl 4-azido-3-iodobenzoate **3**. The 3-iodo functionality in **3** was converted to tributylstannyl moiety in **5** using a palladium catalyst. Alkaline hydrolysis of esters **3** and **5** furnished the corresponding acids **4** and **6,** respectively. Naloxone (**7**) was used as a starting material to prepare azido-opiate probes (**9, 10, 16, 17**) (Scheme 1). First, **7** was converted to β-naloxamine (**8**) using our published method (Majumdar et al. 2011a). Deallylation of **7** using a $Pd(PPh_3)_4$ (Giguere et al. 2012) was employed to obtain noroxymorphone (**11**). Compound **11** was in turn converted to the *N*-propargylamine analog **15** in four steps. *N*-alkylation of **11** with propargyl bromide was followed by stereoselective reduction of the ketone using K-Selectride to yield the α-alcohol **13** (Brossi et al. 1982). The Mitsunobu reaction was employed to convert α-alcohol **13** to β-phthalimide **14** (Váradi et al. 2015). Then, removal of the phthalimide moiety in **14** using hydrazine hydrate in methanol gave the desired *N*-propargyl β–amine **15**. Finally, coupling of *N*-propargyl β–amine **15** or β-naloxamine **8** with acids **4** or **6** using HATU as a coupling reagent afforded the desired azidoaryl probes **9, 10, 16, 17** and. Then, the reaction of the tributyltin precursors **9** or **16** with chloramine-T and $Na^{125}I$ and their semi-preparative purification using reverse

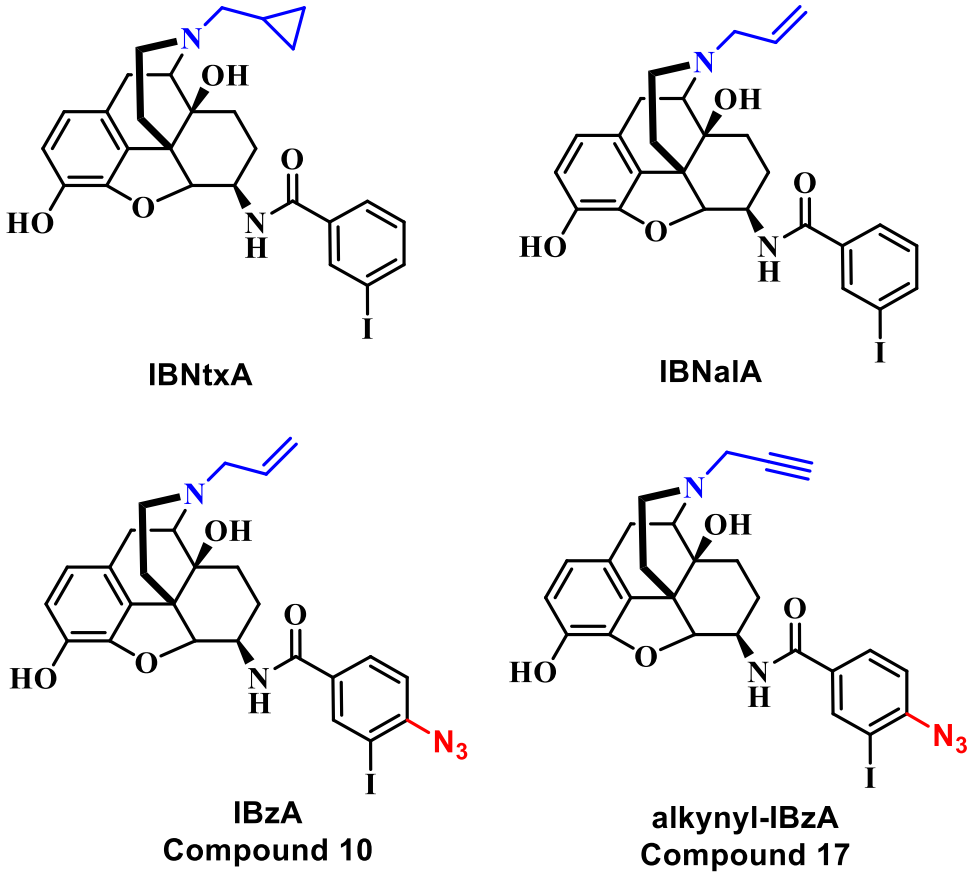

Fig. 1 Chemical structures of IBNtxA, IBNalA and photoaffinity ligands synthesized (IBzA **10**, alkynyl-IBzA **17**)

Table 1 Radioligand ligand binding (K_i, nM) assay

Compound	mMOR-1	mDOR-1	mKOR-1	Triple KO	6TM/E11
IBzA **10**	0.48 ± 0.02	8.3 ± 0.7	0.70 ± 0.20	4.1 [3.5–6.4]	4.64 ± 0.2
Alkynyl-IBzA **17**	0.25 ± 0.12	3.5 ± 0.4	0.92 ± 0.29	0.89 [0.71–1.1]	11.97 ± 1.63
IBNtxA[a]	0.11 ± 0.02	0.24 ± 0.1	0.03 ± 0.001	0.12 ± 0.04	0.16 ± 0.04
IBNalA[a]	0.22 ± 0.12	2.55 ± 0.18	0.08 ± 0.06	nd	0.25 ± 0.12

Each photoaffinity ligand with increasing concentrations was incubated with [^{125}I]-IBNtxA and membranes homogenates from either CHO cells stably expressing mMOR-1, mDOR-1, or mKOR-1, or 6TM/E11 assay (with mMOR-1, mKOR-1 and mDOR-1 blockers added to mouse brain) or triple knockout mouse brain. Results are from at least 3 independent replications and are presented as mean ± SEM except for TKO mouse brain which is a single determination reported as Ki [95% Confidence interval]

nd not determined

[a]Values from literature (Majumdar et al. 2012)

phase HPLC by following the literature procedure afforded [^{125}I]-IBzA **18** and [^{125}I]-Alkynyl-IBzA **19** (Majumdar et al. 2011a).

Two aryl azide photoaffinity labels were synthesized by amide bond coupling of 4-azido-3-iodobenzoic acid and 6-β-naloxonamine (IBzA) or *N*-propargyl-6-β-nornaloxonamine (Alkynyl-IBzA) and their structures validated (Fig. 1).

Pharmacology

Both drugs IBzA **10** and Alkynyl-IBzA **17** displayed a high binding affinity for mMOR-1 and mKOR-1 (mouse kappa opioid receptor transfected in CHO cells) in competition assays, however with a slightly lower affinity for mDOR-1 (mouse delta opioid receptors transfected in CHO cells) by about 10- to 15-fold (Table 1). This kind of selectivity for mMOR-1, mKOR-1 and 6TM/E11 over the mDOR-1 was

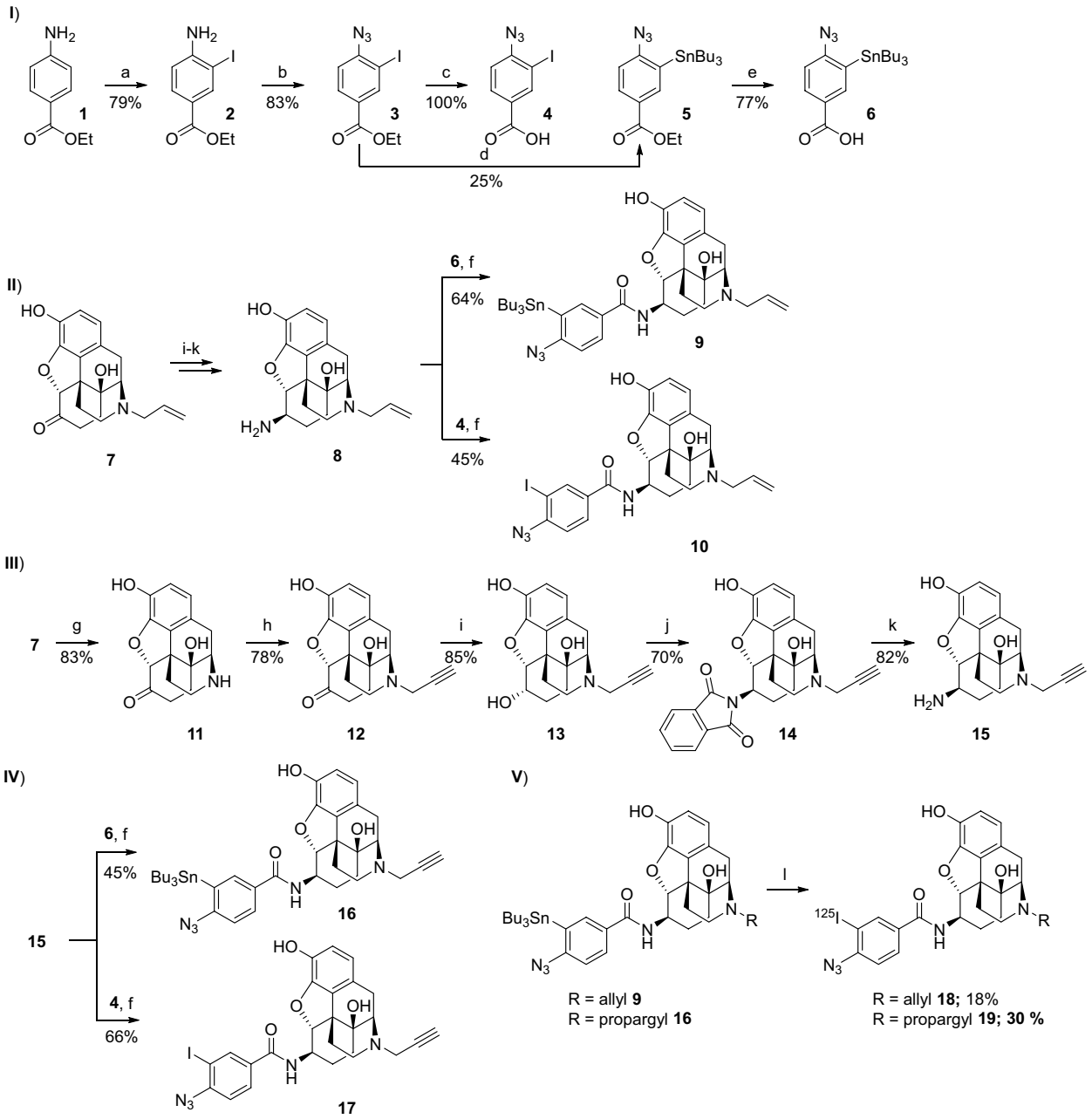

Scheme 1 Reagents and conditions: (a) *N*-iodosuccinimide, Conc. H_2SO_4, acetonitrile, 2 h, rt; (b) Conc. HCl, methyl acetate, aq. $NaNO_2$, 45 min, 4 °C, NaN_3, 30 min, rt; (c) aq. LiOH, MeOH/THF (1:1), 16 h, rt; (d) Bis(tributyltin), $Pd(PPh_3)_4$, dioxane, 16 h, reflux; (e) aq. KOH, MeOH, 16 h, 60 °C; (f) **4** or **6**, HATU, *N*,*N*-diisopropylethylamine (DIEA), DMF, 2 h, 0 °C to rt; (g) *N,N*-dimethylbarbituic acid, $Pd(PPh_3)_4$, DCM, 38 °C, 16 h; (h) Na_2CO_3, propargyl bromide, DMF, 16 h, 90 °C; (i) K-Selectride, THF, 30 min, 0 °C; (j) phthalimide, Ph_3P, THF, diisopropyl azodicarboxylate (DIAD), 16 h, rt; (k) hydrazine hydrate, *cis*-2-penten-1-ol, MeOH, 16 h, rt; (l) Chloramine-T, $Na^{125}I$, MeOH/HOAc/H_2O

seen previously using IBNalA as well. The mMOR-1 affinities of both affinity labels were similar to that of IBNtxA and IBNalA. However, in contrast to both IBNtxA and IBNalA, both affinity labels had lower affinity for 6TM/E11 sites and neither ligand showed any selectivity for 6TM/E11 over the classical opioid receptors. To summarize, the incorporation of 4′-azido group in the aryl ring of IBNalA or IBNtxA led to a diminished 6TM/E11 affinity while retaining high affinity at classical cloned opioid receptors. This unanticipated diminished affinity and selectivity at 6TM/E11 limited their utilization for characterizing this site even though these probes were designed for that purpose. We thereby focused on characterizing the classical opioid receptors and

Table 2 [^{35}S] GTPγS functional assay

Compound	mMOR-1	
	EC_{50} (nM)	E_{max} (%)
IBzA **10**	0.86 ± 0.24	122 ± 3
Alkynyl-IBzA **17**	1.1 ± 0.1	103 ± 3
DAMGO	19 ± 7	100
IBNtxA	0.49 ± 0.12	101 ± 3
IBNalA	1.4 ± 0.3	75 ± 3.5

Efficacy data were obtained using agonist induced stimulation of [^{35}S]GTPγS binding assay. Efficacy is represented as EC_{50} ± SEM (nM) and percent maximal stimulation (E_{max}) ± SEM relative to standard agonist DAMGO (at mMOR-1) at 1000 nM; Results are from 3 independent replications and are presented as mean ± SEM

its complexes in particular focusing on mMOR-1 by using these novel photoaffinity labels.

In [^{35}S]GTPγS functional assays, both IBzA **10** and alkynyl-IBzA **17** were full agonists at MOR-1 (Table 2). Results were found comparable to that of parent compounds IBNtxA and IBNalA in terms of agonistic potency. No efforts were made to characterize these probes at mKOR-1 and mDOR-1 because a limited literature is available on protein complexes of both these subtypes and the efficiency of photochemical coupling of these affinity labels with mKOR-1 in our hands was poor (as described later).

The ^{125}I-radiolabeled versions of these drugs bound to mMOR-1 or mKOR-1 receptors stably expressed in CHO cells with high affinity (Fig. 2). The affinity was greater

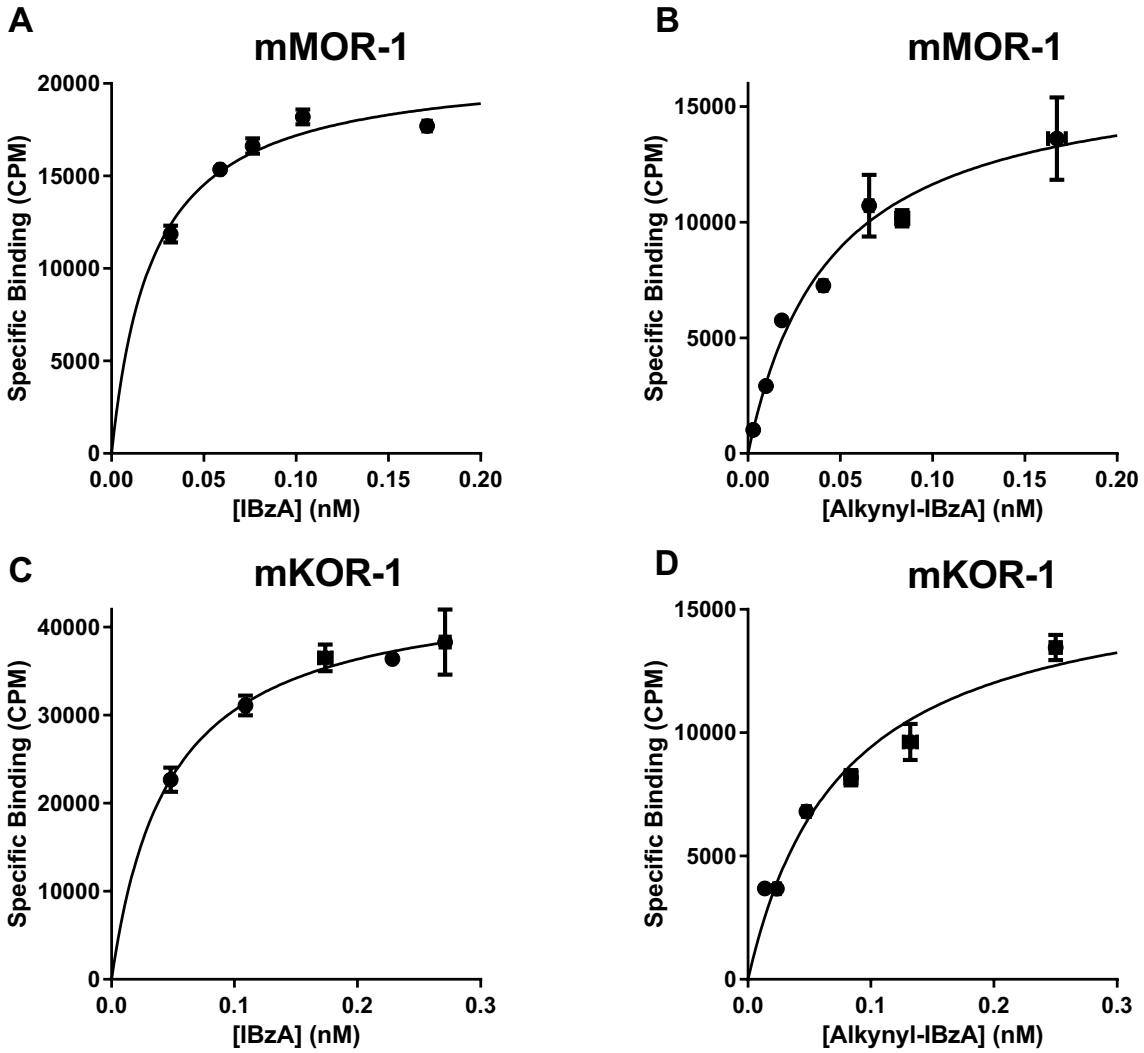

Fig. 2 Saturation binding assays.[^{125}I]-IBzA or [^{125}I]-Alkynyl-IBzA were incubated at the indicated concentrations with membrane homogenate from cells stably transfected with mMOR-1 or mKOR-1. Curves were fit by nonlinear regression using Graphpad Prism. Each study was replicated 3 times and mean values of K_D ± SEM of 3–4 independent replications are presented. There was no significant difference between the K_D values of the drugs at either mMOR-1 or mKOR-1. **a** IBzA, 0.036 ± 0.006 nM at mMOR-1vs, **b** Alkynyl-IBzA, 0.051 ± 0.013 at mMOR-1. **c** IBzA, 0.053 ± 0.002 nM at mKOR-1 vs, **d** Alkynyl-IBzA, 0.056 ± 0.001 nM at mKOR-1

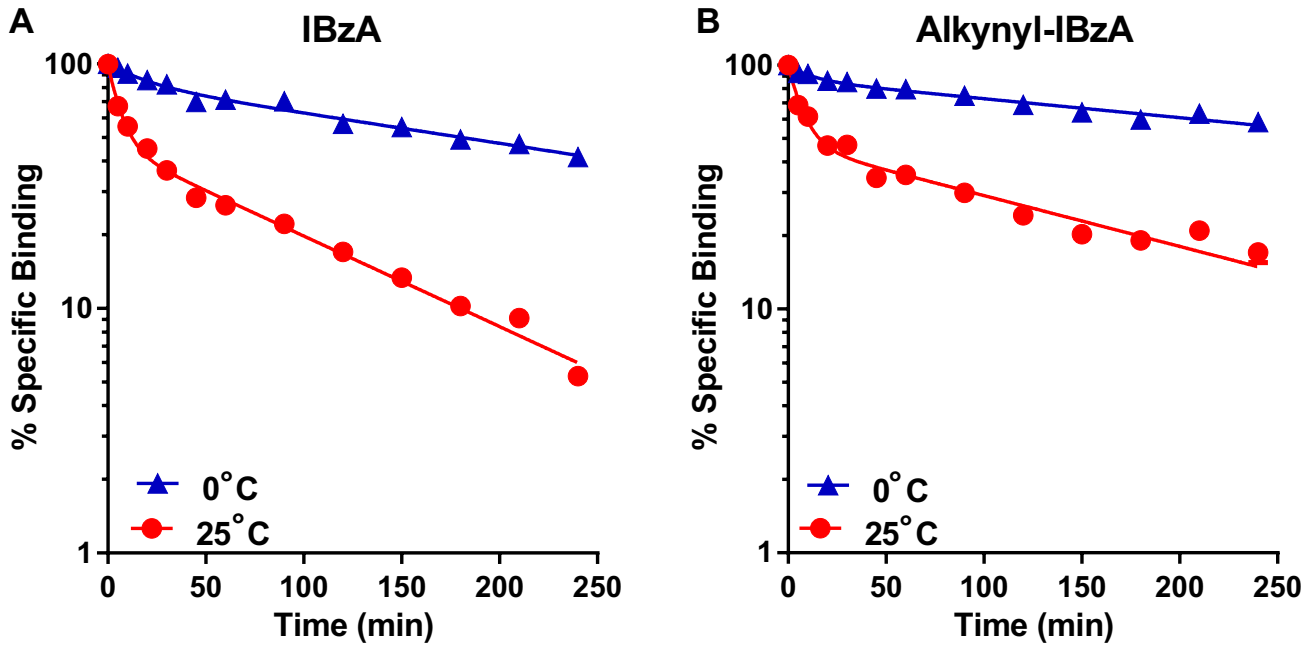

Fig. 3 Dissociation kinetics of binding. Each drug (0.1 nM) was incubated for 1.5 h with mMOR-1/CHO membranes at 25 °C. Levallorphan (10 μM) was then added at the indicated time points (5–240 min) after the 1.5 h incubation to determine the kinetics of drug dissociation. Results are pooled from 3 independent replicates with similar results and are expressed as mean [95% confidence intervals]. **a** The kinetics of dissociation for ^{125}I-IBzA at 25 °C. Data were best fit by a 2-phase exponential decay model ($p < 0.0001$ vs 1-phase decay model, Extra sum of squares F-test), with 53% [51–56%] dissociating rapidly and 47% dissociating very slowly. $\tau_{1/2\ Fast}$: 4.6 min [4.1–5.2 min], $\tau_{1/2\ Slow}$: 81 min [75–89 min]. At 0 °C, the fraction of binding which dissociated slowly was increased to 83% [77–90%] and the dissociation half-life increased to $t_{1/2\ Slow} = 244$ min [207–299 min]. **b** At 25 °C ^{125}I-alkynylIBzA dissociation was best fit by a 2-phase exponential decay model ($p < 0.0001$ vs 1-phase decay model, Extra sum of squares F-test), with 53% [49–56] dissociating rapidly and the remainder very slowly. $\tau_{1/2\ Fast} = 5.2$ min [4.4–6.5 min], $\tau_{1/2\ Slow} = 144$ min [126–169 min]. At 0 °C, the fraction of binding which dissociated slowly was increased to 87% [82–92%] and the dissociation half-life increased to $\tau_{1/2\ Slow} = 389$ min [321–487 min]

than anticipated based upon the competition studies, raising the possibility of two different affinity states of the receptor. This was confirmed in dissociation experiments that revealed the presence of both a rapidly and slowly dissociating component based upon curve fitting of a two-state model (Fig. 3). With both ^{125}I-ligands, approximately half the binding at 25 °C dissociated rapidly and half slowly. Lowering the temperature to 0 °C increased the percentage of slowly dissociating binding to approximately 85%. Since the cell lines expressed a single opioid receptor protein, it seemed likely that the two components in the dissociation curves represented agonist/antagonist conformations of the receptor. To assess this possibility, we examined the effects of the GTP analog GppNHp, which lowers agonist binding affinity (Childers and Snyder 1978). Inclusion of GppNHp virtually eliminated the slowly dissociating component, implying that the radioligands labeled both agonist and antagonist receptor conformations (data not shown).

Both compounds photoaffinity labeled opioid receptors. In mMOR-1-expressing CHO cells, ^{125}I-BzA and ^{125}I-alkynyl-IBzA labeled bands of approximately 65–70 kD (Figs. 4a, 5a), consistent with those from literature (Huang et al. 2015; Lupp et al. 2011). Labeling was found specific, as shown by the absence of the band in the nonspecific lane from tissue in which labeling was carried out in the presence

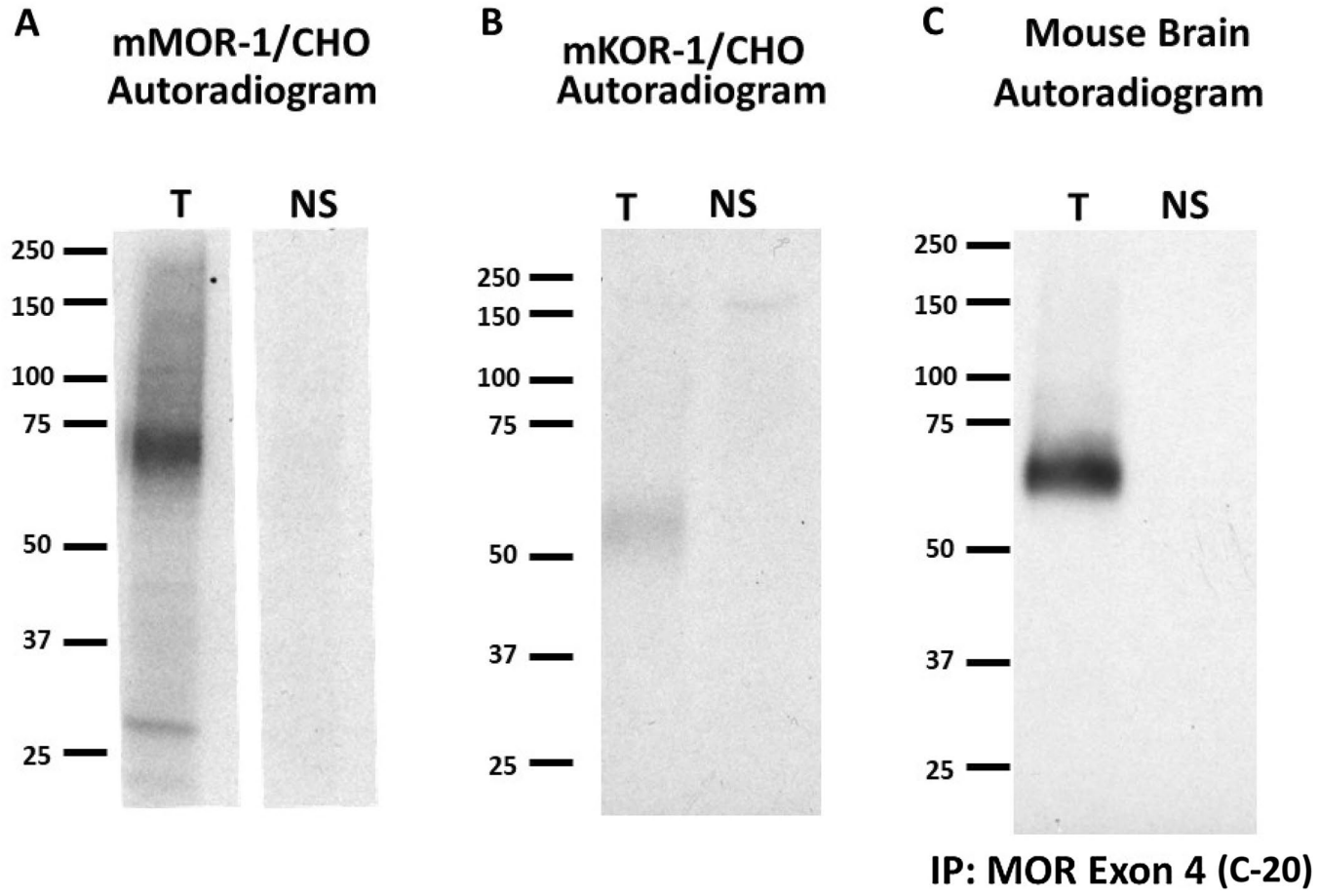

Fig. 4 Photoaffinity labeling with [^{125}I]-IBzA in mMOR-1/CHO, mKOR-1/CHO, and mouse brain. The indicated tissues were photolabeled with [^{125}I]-IBzA and separated by SDS-PAGE. All results have been independently replicated and are representative figures. T, Total; NS, Nonspecific. **a** mMOR-1/CHO. The photolabeled species ran as a diffuse band of approximately 68–75 kDa, consistent with the molecular weight of the mature, glycosylated form of the murine mu opioid receptor. **b** mKOR-1/CHO. mKOR-1 was enriched by wheat germ affinity purification. The photolabeled species ran as a diffuse band of approximately 50–57 kDa, consistent with the molecular weight of the mature, glycosylated form of murine kappa opioid receptor. **c** CD1 Mouse Brain. Mu opioid receptor in mouse brain was photolabeled and enriched by immunoprecipitation with an antibody to the C-terminal region of the receptor. The photolabeled species ran with lower apparent molecular weight than observed in cell lines, approximately 60–65 kDa

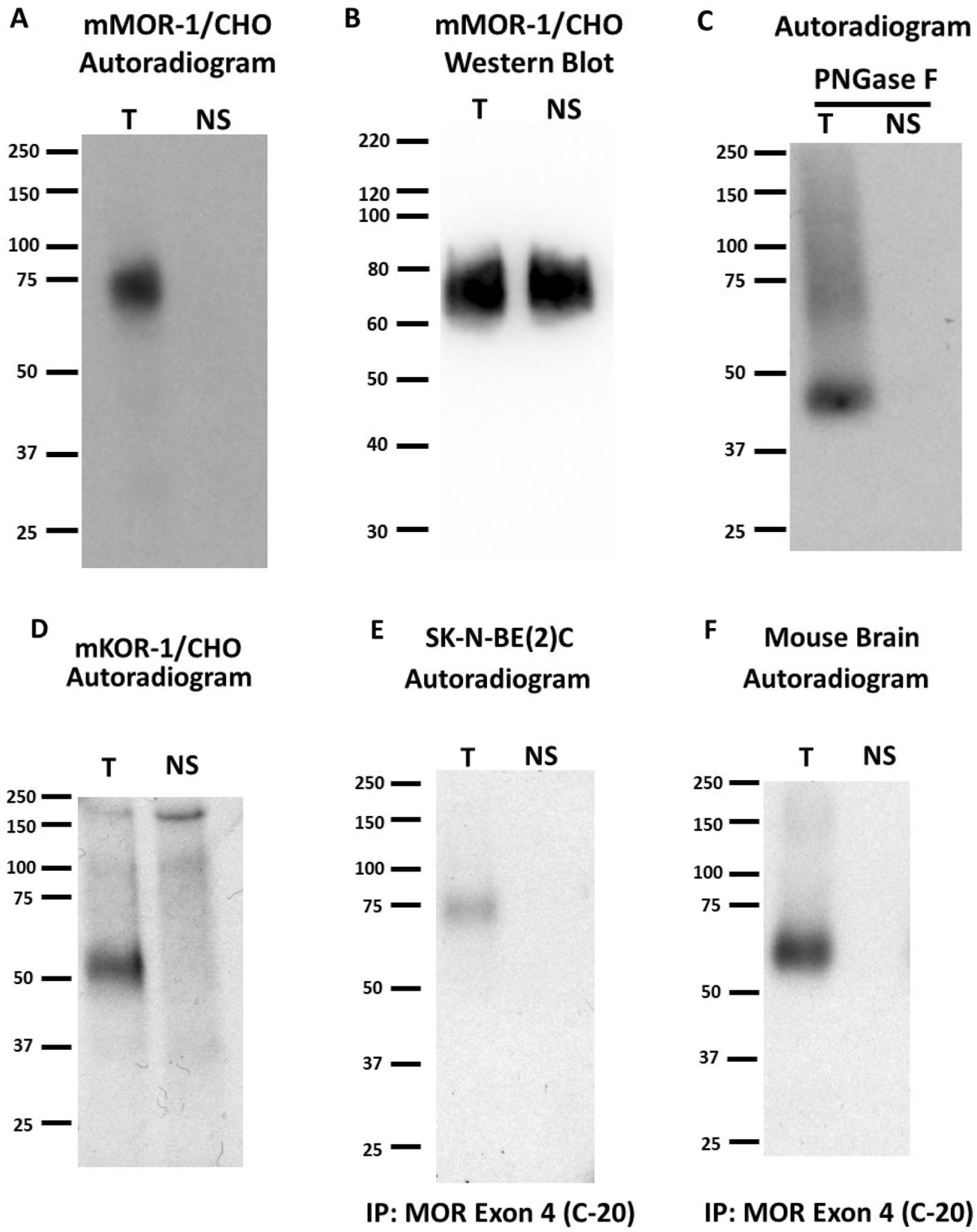
A
mMOR-1/CHO
Autoradiogram
T
NS
250
150
100
75
50
37
25
B
mMOR-1/CHO
Western Blot
T
NS
220
120
100
80
60
50
40
30
C
Autoradiogram
PNGase F
T
NS
250
150
100
75
50
37
25
D
mKOR-1/CHO
Autoradiogram
T
NS
250
150
100
75
50
37
25
E
SK-N-BE(2)C
Autoradiogram
T
NS
250
150
100
75
50
37
25
IP: MOR Exon 4 (C-20)
F
Mouse Brain
Autoradiogram
T
NS
250
150
100
75
50
37
25
IP: MOR Exon 4 (C-20)

◂**Fig. 5** Photoaffinity labeling with [^{125}I]-Alkynyl-IBzA in mMOR-1/CHO, mKOR-1/CHO, and Mouse Brain. The indicated tissues were photolabeled with [^{125}I]-Alkynyl-IBzA and separated by SDS-PAGE. All results have been independently replicated and are representative figures. *T* total; *NS* nonspecific. **a** mMOR-1/CHO. Photolabeled mMOR-1 ran as a diffuse band of approximately 68–75 kDa. **b** mMOR-1 Western Blot. Probing membrane from **a** with MOR-1 antibody confirmed the presence of mMOR-1in both total and nonspecific lanes. **c** PNGaseF treatment. eglycosylation with PNGase F reduced the molecular weight to the predicted molecular weight of 44 kDa. **d** mKOR/CHO. Following Wheat Germ affinity enrichment, photolabeled mKOR-1 ran as a diffuse band from 50–57 kDa. **e** SK-N-BE(2)C neuroblastoma. mMOR-1 were photolabeled in a natively-expressing cell line, appearing as a diffuse band from about 70–77 kDa. **f** C57 Mouse Brain. mMOR-1 in mouse brain ran with a lower apparent molecular weight than observed in cell lines, approximately 57–65 kDa

of levallorphan (1 μM). When using levallorphan (1 μM) that blocks ^{125}I-alkynyl-IBzA binding, the receptor is still present at equivalent protein levels in both total and nonspecific lanes, as shown in the Western blot (Fig. 5b). Cleavage of *N*-linked sugars from the receptor with PNGaseF yielded a photolabeled species with the predicted molecular weight of the mu receptor's amino acid sequence alone, 44 kDa (Fig. 5c).

The expression level of native MOR-1 in mouse brain and SK-N-Be(2)C cells is far lower than in stably transfected cell lines, requiring the addition of an immunoaffinity enrichment step. For MOR-1, we immunopurified the receptor using an antibody raised against an epitope from exon 4 of *Oprm1*. ^{125}I-alkynyl-IBzA specifically labeled a band in mouse brain with 60–70 kDa (Fig. 4c), a size slightly smaller than those seen in mMOR-1-expressing CHO cells (Fig. 4a) and SK-N-Be(2)C that endogenously express mu opioid receptors (Fig. 5e). This is may be due to different glycosylation states of the receptor, as previously reported (Huang et al. 2008). ^{125}I-BzA and ^{125}I-alkynyl-IBzA photolabeled mKOR-1 receptors with significantly lower efficiency, requiring enrichment of the receptor with wheat germ agglutinin affinity chromatography prior to SDS-PAGE (Figs. 4b, 5d). The labeled receptor ran as a diffuse band from about 50–57 kDa (Figs. 4b, 5d), consistent with the early report (Li et al. 2007).

The MOR-1 associates with many proteins to form a protein complex. We explored mMOR-1-containing protein complex using a blue native PAGE approach that permits the evaluation of the receptor complex in relative native states (Schagger et al. 1994; Schagger and

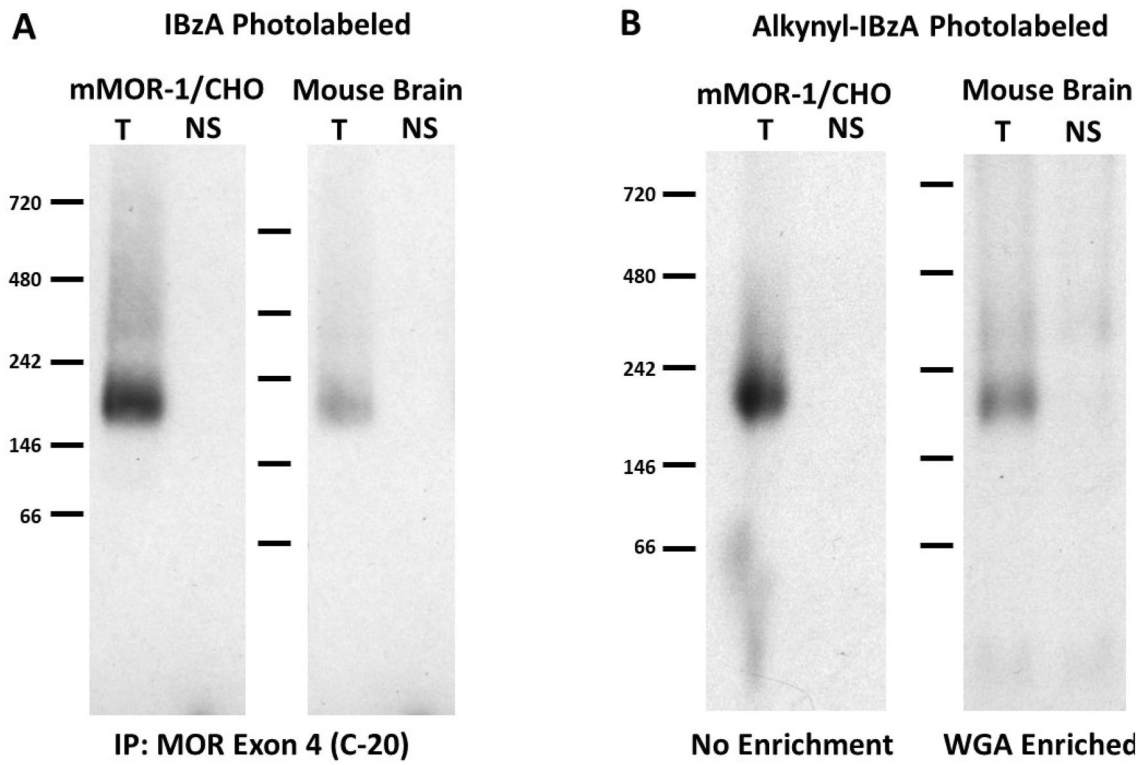

Fig. 6 BN-PAGE of Photoaffinity labeled mMOR-1. **a** mMOR-1/CHO and mouse brain membranes were photolabeled with IBzA and immunoprecipitated under nondenaturing conditions before separation by blue native PAGE to yield a single diffuse band with an approximate molecular weight of 200–220 kDa. **b** mMOR-1/CHO membranes were photolabeled with Alkynyl-IBzA and resolved by BN-PAGE with no enrichment; a simple wheat germ agglutinin enrichment step was added to visualize the species in mouse brain tissue photolabeled with Alkynyl-IBzA. Results have each been independently replicated and are representative autoradiograms

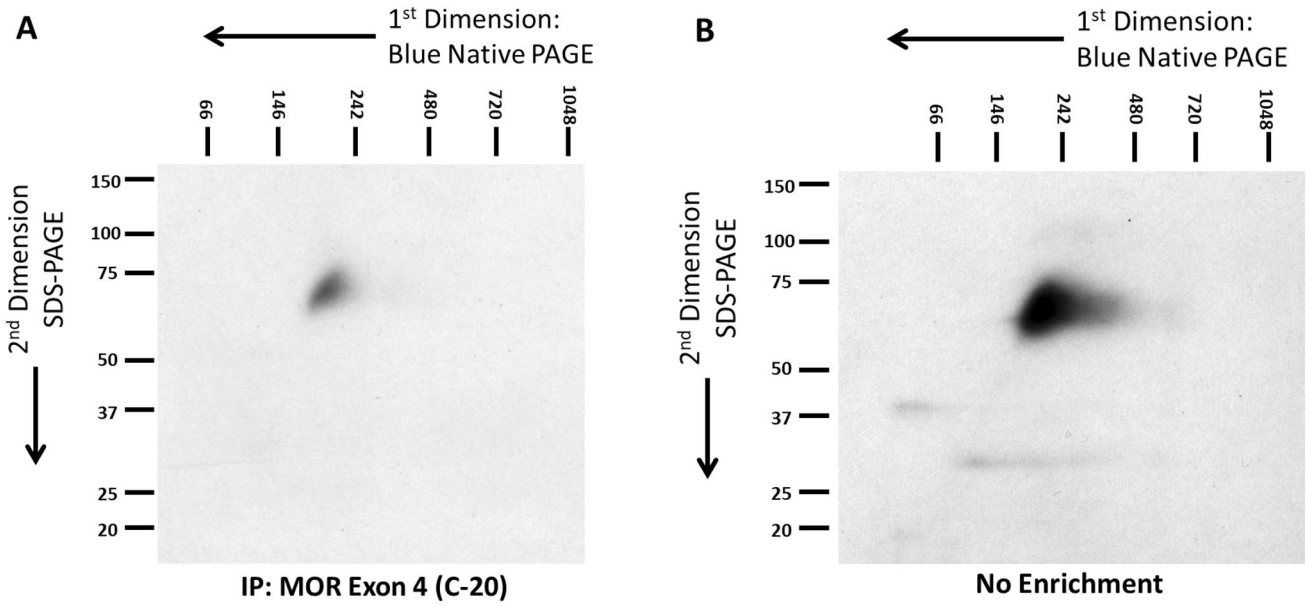

Fig. 7 B2D BN-PAGE/SDS-PAGE. After photolabeling and BN-PAGE separation, a gel lane was excised and run on a denaturing and reducing SDS-PAGE gel in an orthogonal direction. The higher molecular weight band observed by BN-PAGE migrated at approximately 70–75 kDa following SDS-PAGE, consistent with our previous observations for the mu receptor. Results have each been independently replicated and are representative autoradiograms. **a** IBzA photolabeled mMOR-1/CHO membranes, immunoprecipitated under non-denaturing conditions. **b** Alkynyl-IBzA photolabeled mMOR-1/CHO membranes with no enrichment step

von Jagow 1991). On blue native PAGE, ^{125}I-BzA and ^{125}I-alkynyl-IBzA both specifically labeled bands with molecular weights of approximately 200 kDa in mMOR-1-expressing CHO cells and mouse brain (Fig. 6). A second dimension SDS-PAGE under denaturing conditions showed that the radiolabelled bands with 200 kDa were separated into bands with 70–75 kDa in size (Fig. 7) that were similar to those seen in one-dimension SDS-PAGE (Figs. 4, 5). These results suggest that mMOR-1 exists as a protein complex with ~ 200 kDa in size under the conditions we used. The composition of the complex, however, remains unclear. MOR-1 may form homodimers based upon its published crystal structure (Manglik et al. 2012) and may contribute to the complex, although these need to be validated. Perhaps Sigma$_1$ receptors (~ 25 kDa) could also be included within the complex since they tend co-immunoprecipitate with MOR-1 (Kim et al. 2010). It will be interesting to further explore mMOR-1-containing protein complex using IP-crosslinking-proteomics approach.

In conclusion, we have synthesized two photoaffinity labels targeting mMOR-1 and mKOR-1. Future studies will utilize the *N*-propargyl group on alkynyl-IBzA to CLICK arms to purify the target. The ability to keep the receptor complex intact, as shown by blue native PAGE suggests that it may be feasible to purify the complex and define its components.

Author contributions SG and SM jointly supervised this work. SGG, RU, AV, JS and AH performed research and provided tool compounds. SGG, RU, YXP, GWP and SM analyzed data. SGG, RU, GWP and SM wrote the paper with input from all authors. All authors read and approved the final manuscript.

Funding SM is supported by funds from NIH Grants DA045884 and W81XWH-17-1-0256 (Office of the Assistant Secretary of Defense for Health Affairs through the Peer Reviewed Medical Research Program) and start-up funds from Center for Clinical Pharmacology, St. Louis College of Pharmacy and Washington University to SM. This research was funded in part through the NIH/NCI Cancer Center Support Grant P30 CA008748. Studies were also supported by NIDA grants DA042888 and DA046714 (YXP) and DA048379, DA007242 and DA006241 (GWP/YXP).

Compliance with Ethical Standards

Conflict of interest GWP, YXP and SM are co-founders of Sparian BioSciences. All authors report no other biomedical financial interests or potential conflicts of interest.

Ethical Approval All applicable international, national, and/or institutional guidelines for the care and use of animals were followed. This article does not contain any studies with human participants or animals performed by any of the authors.

References

Best MD (2009) Click chemistry and bioorthogonal reactions: unprecedented selectivity in the labeling of biological molecules. Biochemistry 48:6571–6584

Bochet P, Icard-Liepkalns C, Pasquini F, Garbay-Jaureguiberry C, Beaudet A, Roques B, Rossier J (1988) Photoaffinity labeling of opioid d receptors with an iodinated azido-ligand: [^{125}I]D-Thr^{2}, p_N3Ph^{e}4, L^{e}u5]enkephalyl-T^{h}r6. Mol Pharmacol 34:436–443

Bolan EA, Pan YX, Pasternak GW (2004) Functional analysis of MOR-1 splice variants of the mouse mu opioid receptor gene Oprm. Synapse 51:11–18. https://doi.org/10.1002/syn.10277

Brossi A, Hsu FL, Rice KC (1982) A simplified synthesis of (+)-4-hydroxy-N-methylmorphinan-6-one. J Organ Chem 47:5214–5216. https://doi.org/10.1021/jo00147a039

Chae PS et al (2010) Maltose-neopentyl glycol (MNG) amphiphiles for solubilization, stabilization and crystallization of membrane proteins. Nat Methods 7:1003–1008. https://doi.org/10.1038/nmeth.1526

Cheng Y-C, Prusoff WH (1973) Relationship between the inhibition constant (K1) and the concentration of inhibitor which causes 50 percent inhibition (I50) of an enzymatic reaction. Biochem Pharmacol 22:3099–3108

Childers SR, Snyder SH (1978) Guanine nucleotides differentiate agonist and antagonist interactions with opiate receptors. Life Sci 23:759–762

Chou T-C (1974) Relationships between inhibition constants and fractional inhibition in enzyme-catalyzed reactions with different numbers of reactants, different reaction mechanisms, and different types and mechanisms of inhibition. Mol Pharmacol 10:235–247

Clarke S, Chen ZP, Hsu MS, Pintar J, Hill R, Kitchen I (2001) Quantitative autoradiographic mapping of the ORL1, m-, d- and kappa-receptors in the brains of knockout mice lacking the ORL1 receptor gene. Brain Res 906:13–24

Giguere JR, McCarthy KE, Reisch HA, Sandoval S, Stymiest JL (2012) Transition metal-catalyzed processes for the preparation of N-allyl compounds and use thereof. US patent US9624232B2

Grinnell SG, Majumdar S, Narayan A, Le Rouzic V, Ansonoff M, Pintar JE, Pasternak GW (2014) Pharmacologic characterization in the rat of a potent analgesic lacking respiratory depression, IBNtxA. J Pharmacol Exp Ther 350:710–718. https://doi.org/10.1124/jpet.114.213199

Huang P et al (2008) Brain region-specific N-glycosylation and lipid rafts association of the rat mu opioid receptor. Biochem Biophys Res Commun 365:82–88

Huang P, Chen C, Liu-Chen LY (2015) Detection of mu opioid receptor (MOPR) and its glycosylation in rat and mouse brains by western blot with anti-muC, an affinity-purified polyclonal anti-MOPR antibody. Methods Mol Biol 1230:141–154. https://doi.org/10.1007/978-1-4939-1708-2_11

Kim FJ, Kovalyshyn I, Burgman M, Neilan C, Chien CC, Pasternak GW (2010) Sigma 1 receptor modulation of G-protein-coupled receptor signaling: potentiation of opioid transduction independent from receptor binding. Mol Pharmacol 77:695–703. https://doi.org/10.1124/mol.109.057083

Li JG, Chen C, Liu-Chen LY (2007) N-Glycosylation of the human kappa opioid receptor enhances its stability but slows its trafficking along the biosynthesis pathway. Biochemistry 46:10960–10970. https://doi.org/10.1021/bi700443j

Lupp A, Richter N, Doll C, Nagel F, Schulz S (2011) UMB-3, a novel rabbit monoclonal antibody, for assessing mu-opioid receptor expression in mouse, rat and human formalin-fixed and paraffin-embedded tissues. Regul Pept 167:9–13. https://doi.org/10.1016/j.regpep.2010.09.004

Majumdar S, Burgman M, Haselton N, Grinnell S, Ocampo J, Pasternak AR, Pasternak GW (2011a) Generation of novel radiolabeled opiates through site-selective iodination. Bioorg Med Chem Lett 21:4001–4004. https://doi.org/10.1016/j.bmcl.2011.05.008

Majumdar S et al (2011b) Truncated G protein-coupled mu opioid receptor MOR-1 splice variants are targets for highly potent opioid analgesics lacking side effects. Proc Natl Acad Sci USA 108:19778–19783. https://doi.org/10.1073/pnas.1115231108

Majumdar S et al (2012) Synthesis and evaluation of aryl-naloxamide opiate analgesics targeting truncated exon 11-associated mu opioid receptor (MOR-1) splice variants. J Med Chem 55:6352–6362. https://doi.org/10.1021/jm300305c

Manglik A et al (2012) Crystal structure of the mu-opioid receptor bound to a morphinan antagonist. Nature 485:321–326. https://doi.org/10.1038/nature10954

Pan YX (2003) Expression of opioid receptors in mammalian cell lines. Methods Mol Med 84:17–28

Pasternak GW, Pan Y-X (2013) Mu opioids and their receptors: evolution of a concept. Pharmacol Rev 65:1257–1317. https://doi.org/10.1124/pr.112.007138

Schagger H, von Jagow G (1991) Blue native electrophoresis for isolation of membrane protein complexes in enzymatically active form. Anal Biochem 199:223–231

Schagger H, Cramer WA, von Jagow G (1994) Analysis of molecular masses and oligomeric states of protein complexes by blue native electrophoresis and isolation of membrane protein complexes by two-dimensional native electrophoresis. Anal Biochem 217:220–230

Schuller AG et al (1999) Retention of heroin and morphine-6 beta-glucuronide analgesia in a new line of mice lacking exon 1 of MOR-1. Nat Neurosci 2:151–156. https://doi.org/10.1038/5706

Sumranjit J, Chung SJ (2013) Recent advances in target characterization and identification by photoaffinity probes. Molecules 18:10425–10451. https://doi.org/10.3390/molecules180910425

Takayanagi I, Shibata R, Miyata N, Hirobe M (1982) Photoaffinity labeling of opioid receptor with morphine-7,8-oxide (morphine epoxide). J Pharmacol Methods 7:185–192

Thirumurugan P, Matosiuk D, Jozwiak K (2013) Click chemistry for drug development and diverse chemical-biology applications. Chem Rev 113:4905–4979. https://doi.org/10.1021/cr200409f

Váradi A et al (2015) Synthesis and characterization of a dual kappa-delta opioid receptor agonist analgesic blocking cocaine reward behavior. ACS Chem Neurosci 6:1813–1824. https://doi.org/10.1021/acschemneuro.5b00153

Varadi A et al (2016) Mitragynine/corynantheidine pseudoindoxyls as opioid analgesics with mu agonism and delta antagonism, which do not recruit beta-arrestin-2. J Med Chem 59:8381–8397. https://doi.org/10.1021/acs.jmedchem.6b00748

Wofsy L, Metzger H, Singer SJ (1962) Affinity labeling-a general method for labeling the active sites of antibody and enzyme molecules. Biochemistry 1:1031–1039

Zhu YX et al (1999) Retention of supraspinal delta-like analgesia and loss of morphine tolerance in d *opioid receptor* knockout mice. Neuron 24:243–252